DSN Telemetry System Performance With Convolutionally Coded Data: Sequential Decoding Update

C. A. Greenhall
DSN Systems Engineering Office

DSN Telemetry System performance in decoding convolutionally coded data by both sequential and maximum-likelihood techniques is being determined by testing at various Deep Space Stations. This article describes corrections and refinements to the sequential decoding tests.

I. Introduction

Reference 1 described an ongoing program of tests designed to measure the performance of the DSN on convolutionally coded data. Both sequential and maximum-likelihood decoding techniques were tested. The former is used by the Pioneer and Helios projects, and the latter will be used by Mariner Jupiter–Saturn.

The present article is an update of Ref. 1 in the area of sequential decoding. It describes changes in the offline decoding program, improved estimates of signal-to-noise ratio (SNR), progress toward the determination of optimal modulation indexes, and comparisons between online and offline decoding tests.

II. Changes in the Decoding Algorithm

Since Ref. 1 was written, we have made some corrections to our offline sequential decoding algorithm to bring it more into line with the program in the Data Decoder Assembly (DDA) and to eliminate undetected bit errors. All test files were redecoded with the corrected program. The corrections are:

(1) A computation is counted when either the decoder steps forward along a best branch, or the decoder steps backward and does not immediately step forward again. Sideward steps are not counted. (A sideward step is a backward step along a best branch followed by a forward step along a worst

branch.) This change improved the comparison between online and offline decoding tests.

(2) The known bits in the tail (usually the last 32 bits of each frame) are "forced." In other words, the code tree ceases to branch once the tail is reached. Furthermore, the threshold is not tightened while the decoder is in the tail. This forces the decoder to back directly out of the tail if it turns out that errors were made in the bits immediately before the tail. This handling of the tail[1] eliminated the undetected bit errors reported in Ref. 1.

III. Tabular Summary of Tests

Each block of tests in Table 1 identifies a particular bit rate. The "nominal cutoff" is the nominal DDA sequential decoding computation rate of 20480 computations per second, referred to the given bit rate.

For each test we show

(a) The modulation index (MI).

(b) The observed symbol error rate (SER).

(c) The values of total power to noise spectral density ratio (P_t/N_0) and symbol energy to noise spectral density ratio (E_s/N_0) inferred from SER by a method explained in the next section. These are estimates of SNR before system degradations.

(d) Frame deletion rates for online and offline tests at the nominal cutoff. Where both online and offline deletion rates are shown, the two types of tests were run either at the same time or one right after the other. For blocks A to E, the SER was taken from the offline tests. The Block F online tests were performed at DSS 62, Madrid, Spain; for these tests, SER was available.

The frame length for the online tests is 192 bits; for the offline tests it is 180 bits (since the offline decoding program requires frame length to be a multiple of 36). An exception is test B1, where both online and offline tests use an 1152-bit frame. All tests use a 32-bit tail sequence.

For the cases with at least 10 deletions, an estimate of standard error is given. If there are k deletions, the error is $100/\sqrt{k}$ % of the deletion rate.

[1]Suggested by J. W. Layland.

IV. Inference of Signal-to-Noise Ratio

As Ref. 1 noted, it has been difficult to determine the value of P_t/N_0 at the receiver. We therefore presented results using observed symbol error rate as an indicator of test conditions. (Decoder bit energy to noise spectral density ratio (E_b/N_0) was deduced by inverting the complementary error function.) For the present report, we ran a telemetry analysis program[2] with trial values of E_s/N_0 and observed the output SER. Using our *measured* SER, we could interpolate a value for input E_s/N_0 and, hence, for P_t/N_0.

Figure 1 shows the inferred P_t/N_0 versus modulation index for test blocks A through F.

It will be rather difficult to determine optimum modulation indexes from the tests run so far, for one does not find many tests with nearly the same P_t/N_0 but different modulation indexes. The next section discusses the conclusions that can be drawn about goodness of modulation indexes.

V. Choice of Modulation Indexes

Figure 2 shows sample distribution functions of the number of computations per bit for selected tests. Each vertical line is an approximate 90% confidence interval for the value of the distribution function. If p is the value of the function, and there are a total of n data, the confidence interval is

$$p\left(1 \pm \frac{1.65}{\sqrt{np}}\right)$$

We use this formula only for $np \geq 10$ data.

Referring to Figs. 1 and 2, we consider each test block (data rate) in turn.

Block A—2048 bits/s

Test A6 has lower power than A2 or A7, yet the A6 curve is lower than the others. It is not much lower, but the hypothesis that the A6 curve is above the A2 curve (at one point) is rejected by a statistical test at the 90% level. Thus, an MI of 67.6 deg is better than 55 or 75 deg.

Block B—1024 bits/s

B6 has less power than B3 or B7, and its curve is lower. Again, 67.6 deg is better than 55 or 75 deg.

[2]Written by G. Dunn.

Block C—128 bits/s

C4 has about 0.1 dB more power than C2, but the C2 curve is below the C4 curve up to 20 computations/bit. Beyond 20, there are not enough data, and we cannot say anything about the deletion rate at the nominal cutoff of 160 computations/bit. Nevertheless, it appears that 55 deg is better than 42 deg.

Block D—64 bits/s

D4 has more power than D1, but D4's performance is much poorer. An MI of 42 deg is simply much too low here—there is not enough power in the data.

D6 has more power than D5, but D6 is useless for telemetry. The shape of the distribution near its left end does not give a hint of the extremely heavy tail. It appears that an MI of 66.5 deg is much too high. There is not enough power in the carrier, and receiver phase jitter causes symbol errors to appear in bursts. Large numbers of computations become more likely.

Block E—16 bits/s

E5 has more power than E1, and its MI is higher. Although it is impossible to predict which would have the higher deletion rate at 1280 computations/bit, the curve for E5 appears to have the heavy tail characteristic of an MI that is too high. We cannot choose between 42 and 45 deg here.

The E3 and E4 curves show identical performance from MIs of 37.2 and 42 deg.

Block F—8 bits/s

The obvious comparisons—F2 with F5, and F3 with F4—fail to show any advantage of one MI over another.

Comments. We can make some qualitative remarks about the effect of modulation index on the distribution of computations. If MI is too low, the distribution curve has a knee near 1 computation/bit. Nearly perfect frames are unlikely because the SER is high. As MI increases, the knee disappears, the slope of the curve becomes steeper, and the curve approximates a Pareto ($x^{-\alpha}$) distribution. The optimum MI is probably found in this range. As MI continues to increase, the curve becomes convex. Although the initial part of the curve is not much affected, the tail of the distribution becomes heavier as receiver phase jitter causes the symbol errors to become dependent.

We have not been able to pin down a clear optimum MI (within, say 1 deg) for any of these bit rates. This is partly because the P_t/N_0 values did not come out as intended. What is needed is a sequence of tests in which the Y-factor, which controls P_t/N_0, is kept accurately constant for a whole sequence of tests, while the MI is varied from test to test. It does not matter that it is difficult to relate *true* P_t/N_0 to the *observed* Y-factor. The true P_t/N_0 can be estimated later as we did in Section IV or by using the Symbol Synchronizer Assembly estimate of E_s/N_0. The important thing is that P_t/N_0 be kept constant (whatever its value) while varying MI.

VI. Comparison of Online and Offline Sequential Decoding

Purposes of offline decoding tests are (a) to measure performance when parameters such as frame length, tail length, and deletion cutoff are changed, and (b) to detect when something is seriously wrong with the online tests and to provide a backup in this case. It is thus necessary to find out how well the offline decoding program simulates the DDA decoder. Figure 3 shows some comparison plots, with some 90% confidence intervals attached to the distribution curves. The functions never disagree by more than a factor of 4 (until the statistics become unreliable). The offline B1 (frame length 1152) distribution function has more of a knee than the online function, but otherwise tracks the online function faithfully.

Since the offline tests are under better control than the online tests, we have rejected those online tests whose distribution curves differ *radically* from those of the corresponding offline tests. For example, as Table 1 shows, we rejected all Block D online tests except D6.

For Block F, however, the *offline* tests were rejected. It was difficult to get enough data at this low rate, and results differed widely from run to run.

Reference

1. Mulhall, B. D. L., *et al.*, "DSN Telemetry System Performance With Convolutionally Coded Data," in *The Deep Space Network Progress Report 42-30*, pp. 184–199, Jet Propulsion Laboratory, Pasadena, Calif., Dec. 15, 1975.

Table 1. Telemetry conditions and deletion rates

Test label	Modulation index, deg	SER, %	P_t/N_0, dB s^{-1}	E_s/N_0, dB	Deletion rate ($\times 10^{-4}$) Online	Offline
Block A. 2048 bits/s; nominal cutoff 10 computations/bit						
1	55.0	6.19	38.79	0.93		150 ± 6%
2	55.0	4.58	39.57	1.71	6.0 ± 25%	2.0
3	55.0	4.09	39.82	1.96	59 ± 8%	2.5
4	55.0	3.21	40.35	2.49	1.8	0.5
6	67.6	3.50	39.24	2.43	24 ± 13%	0.4
7	75.0	3.12	39.27	2.85	2.0	4.2 ± 30%
Block B. 1024 bits/s; nominal cutoff 20 computations/bit						
1[a]	55.0	6.99	35.55	0.70	33 ± 20%	44 ± 30%
2	55.0	5.84	36.05	1.20		6.7 ± 30%
3	55.0	3.92	37.00	2.15	5.6 ± 30%	10 ± 20%
4	55.0	3.11	37.49	2.64		0
6	67.6	3.47	36.40	2.61		0
7	75.0	3.16	36.53	3.12		6.1
Block C. 128 bits/s; nominal cutoff 160 computations/bit						
1	55.0	4.56	28.33	2.51	0	0
2	55.0	3.33	28.97	3.15	0.8	<2.5
3	55.0	2.33	29.60	3.78	0	0
4	42.0	5.88	29.09	1.52	3.0	<1
Block D. 64 bits/s; nominal cutoff 320 computations/bit						
1	55.0	3.70	26.25	3.45		<5
2	55.0	2.99	26.63	3.83		0
3	55.0	1.61	27.60	4.80		0
4	42.0	5.77	26.43	1.87		20 ± 30%
5	58.4	2.06	27.16	4.69		0
6	66.5	2.52	27.22	5.40	45 ± 35%	124 ± 12%
Block E. 16 bits/s; nominal cutoff 1280 computations/bit						
1	42.0	6.8	21.2	2.7		7
3	42.0	~3.0	~22.7	~4.2		<10
4	37.2	3.88	22.86	3.44		0
5	45.0	4.56	21.80	3.74		<17
Block F. 8 bits/s; nominal cutoff 2560 computations/bit						
1	42.0	6.43	19.36	3.83	13	
2	42.0	4.14	20.03	4.50	0	
3	42.0	2.69	20.66	5.13	0	
4	37.2	3.73	20.62	4.21	0	
5	45.0	3.10	20.31	5.26	2.0	

[a]Frame length = 1152 bits.

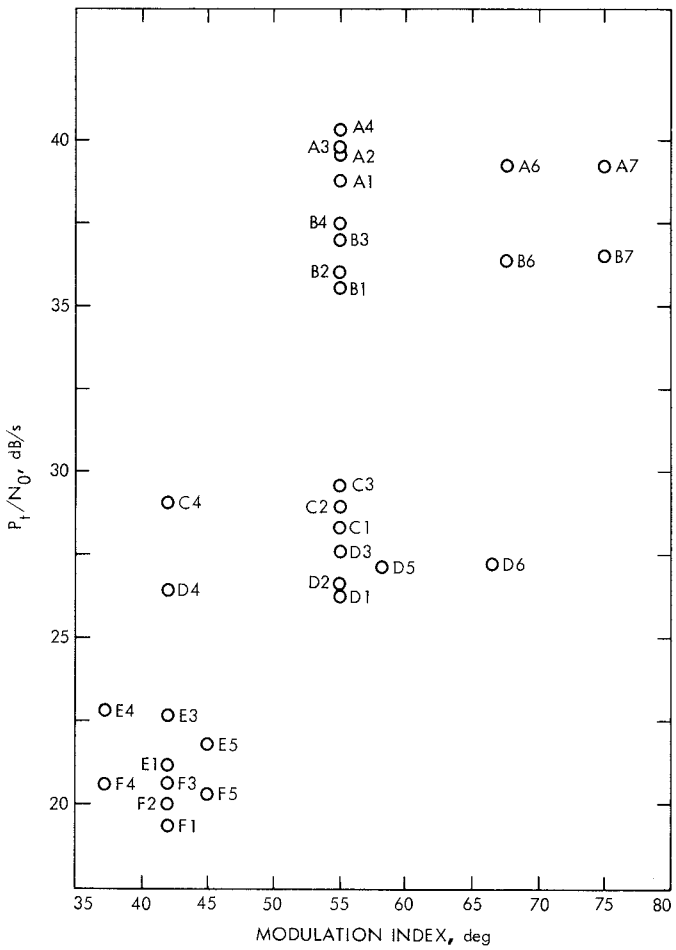

Fig. 1. Test conditions

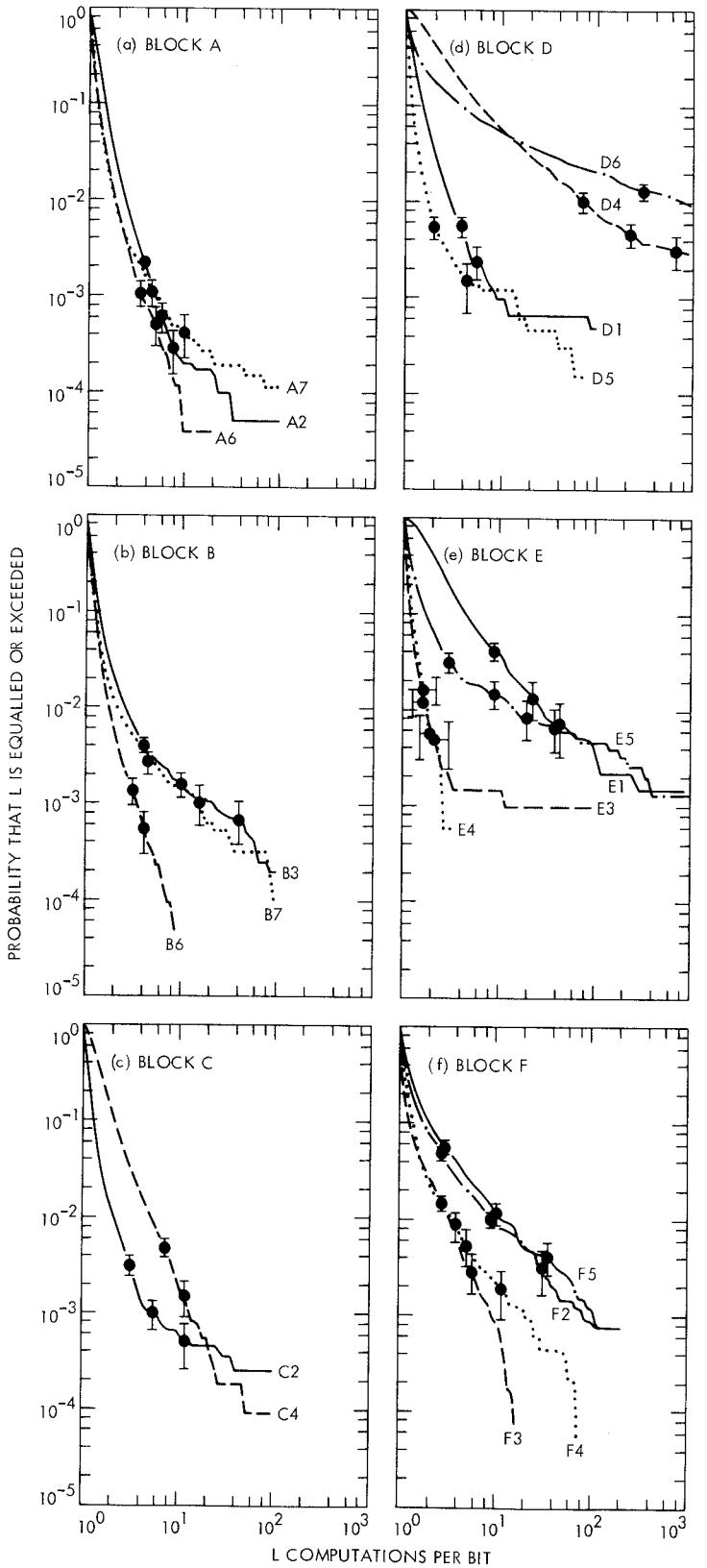

Fig. 2. Sample distribution functions of computations per bit

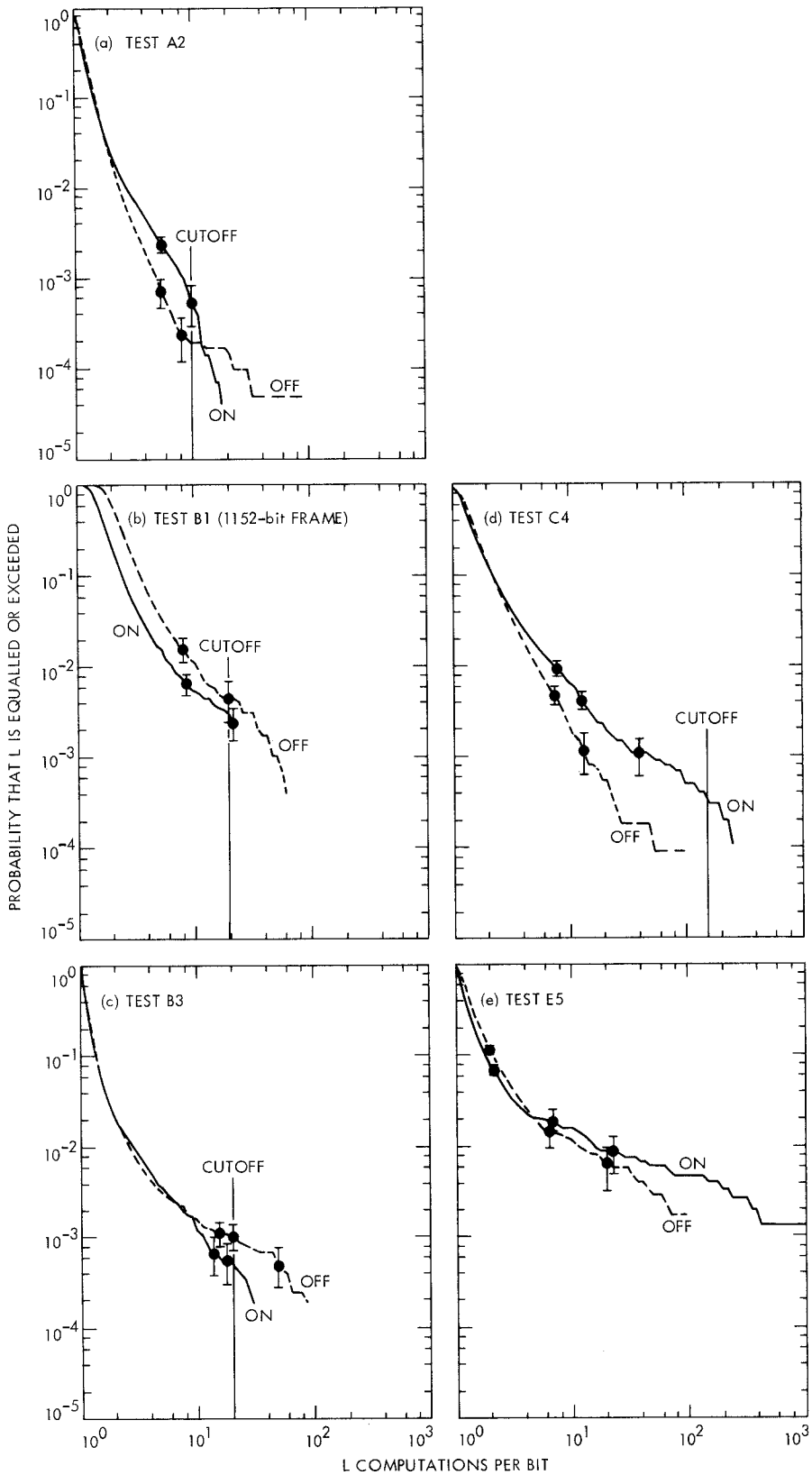

Fig. 3. Online and offline sequential decoding